J Solid State Electrochem (2009) 13:1591–1597
DOI 10.1007/s10008-008-0740-y

ORIGINAL PAPER

Facile fabrication of porous NiO films for lithium-ion batteries with high reversibility and rate capability

Qinmin Pan · Jia Liu

Received: 9 October 2008 / Revised: 24 October 2008 / Accepted: 8 November 2008 / Published online: 2 December 2008

Abstract We report the high-rate capability and good cyclability of three-dimension nanoporous NiO films as the anodes of lithium-ion batteries. The NiO films are fabricated by immersing foam nickel substrates in an 80 °C aqueous solution containing ammonia and potassium peroxydisulfate, and subsequent heat treatment at 500 °C. At a rate of 1.0 C, the film electrodes maintain a capacity of 560 mAh g^{-1} as well as capacity retention of 97% after 100 discharge/charge cycles. When the current density is increased to 14C, 42% of the capacity can be retained. Owing to the ease of large-scale fabrication and superior electrochemical performance, these NiO films will be promising anodes for high-energy-density lithium-ion batteries.

Keywords NiO films · Foam nickel substrate · Solution immersion · High reversibility and rate capability · Lithium-ion batteries

Introduction

The increasing demand for high-energy-density power sources has stimulated intensive exploration of new electrode materials for lithium-ion batteries [1, 2]. Among a variety of alternative anode materials being studied, transition metal oxides (MO, M = Fe, Co, Ni, Cu, etc.) are one family of anode materials with high storage capacity and good safety [3, 4]. These MO exhibit a conversion storage mechanism that takes place in nanocrystalline oxides, instead of intercalation mechanism of the conventional carbonaceous materials. However, the practical use of these materials has been frustrated by their fast capacity fading upon cycling, due to the severe volume changes that occur during lithium insertion/extraction process, as well as poor electronic conductivity.

To improve the electrochemical performance of MO, structuring material in the nanoscale has been attracted considerable attention. Beside the large contact area with electrolyte, nanostructured materials shorten Li ion diffusion path, leading to enhanced power density compared to bulk counterparts [5]. For example, batteries fabricated from nanostructured V_2O_5 [6], Fe_3O_4 [7], Co_3O_4 [8], and TiO_2 [9] have shown very high power densities. In addition, forming composite materials is another approach to enhance cycling performance [10, 11]. But this method will further increase the complexity of material processing and reduce the specific capacity due to the introduction of less electroactive materials. Recently, three-dimensional porous MO electrodes have been suggested for improving cycling performance and rate capability, because they could efficiently transport charge carriers while maintaining a large contact area with electrolyte [12, 13]. Nevertheless, fabricating these porous electrodes involved either complicated equipments or tedious procedures. Therefore a straightforward and efficient fabricating method is required.

As a novel anode material with a theoretical capacity of 718 mAh g^{-1}, NiO shows worse cyclability and rate capability compared to other MO materials [14–19]. This situation is mainly due to the poor electronic conductivity of NiO particles. Despite much effort that had been devoted to cycling characteristics and rate capability improvement, the achievements were not satisfying.

Here, we present a simple method to fabricate nanostructured NiO films on foam nickel substrates for lithium-

Q. Pan (✉) · J. Liu
School of Chemical Engineering and Technology,
Harbin Institute of Technology,
Harbin 150001, People's Republic of China
e-mail: panqm@hit.edu.cn

ion batteries. The NiO films not only share the same advantages as other nanostructured electrodes such as high-electrode/electrolyte contact area, fast lithium-ion diffusion and good strain accommodation [20], but also have the virtues of easy fabrication and low cost. As a result, the films show high reversible capacity, good cyclability and outstanding rate capability as the anodes of lithium-ion batteries.

Experimental

In a typical experiment, foam nickel plates (2 cm×3 cm) were immersed in an aqueous solution contained 0.4 M NH_4OH (25 wt.%) and 0.1 M $K_2S_2O_8$. After the mixture was maintained at 80 °C for 5 h, the foam nickel plates with black color were taken out from the solution and rinsed with distilled water. Then, the plates were heated at 500 °C for 30 min in a quartz-tube under argon atmosphere.

The obtained NiO films were cut into circular plates (φ= 1.0 cm), and then dried in vacuum and weighed. Lithium foils were used as the counter and the reference electrodes. The electrolyte solution was 1.0 M $LiPF_6$ in EC/DMC (1:1 by volume). Coin cells were assembled in a glove-box filled with argon atmosphere. The electrochemical performance of the NiO films was evaluated by galvanostatic discharge–charge between 0 V and 3.0 V using a computer-controlled battery tester. Cyclic voltammograms (CVs) were recorded on a CHI604 potentiostat at a scan rate of 0.5 mV s^{-1}. All the potentials indicated here were referred to the Li/Li^+ electrode potential.

The mass of NiO films deposited on foam nickel substrates was estimated to be about 1.0 mg cm^{-2} according to the procedure described in the literature [21]. Scanning electron microscopy (SEM) images and energy dispersive X-ray analysis (EDX) were obtained with a QUANTA200 (FEI) scanning electron microscope. X-ray photoelectron spectroscopy (XPS, SCALAB2020IXL) measurement was performed in an ultrahigh vacuum (UHV, 2.5×10^{-10}-Torr base pressure) with the use of a monochromatic Al Ka source (1,486.6 eV).

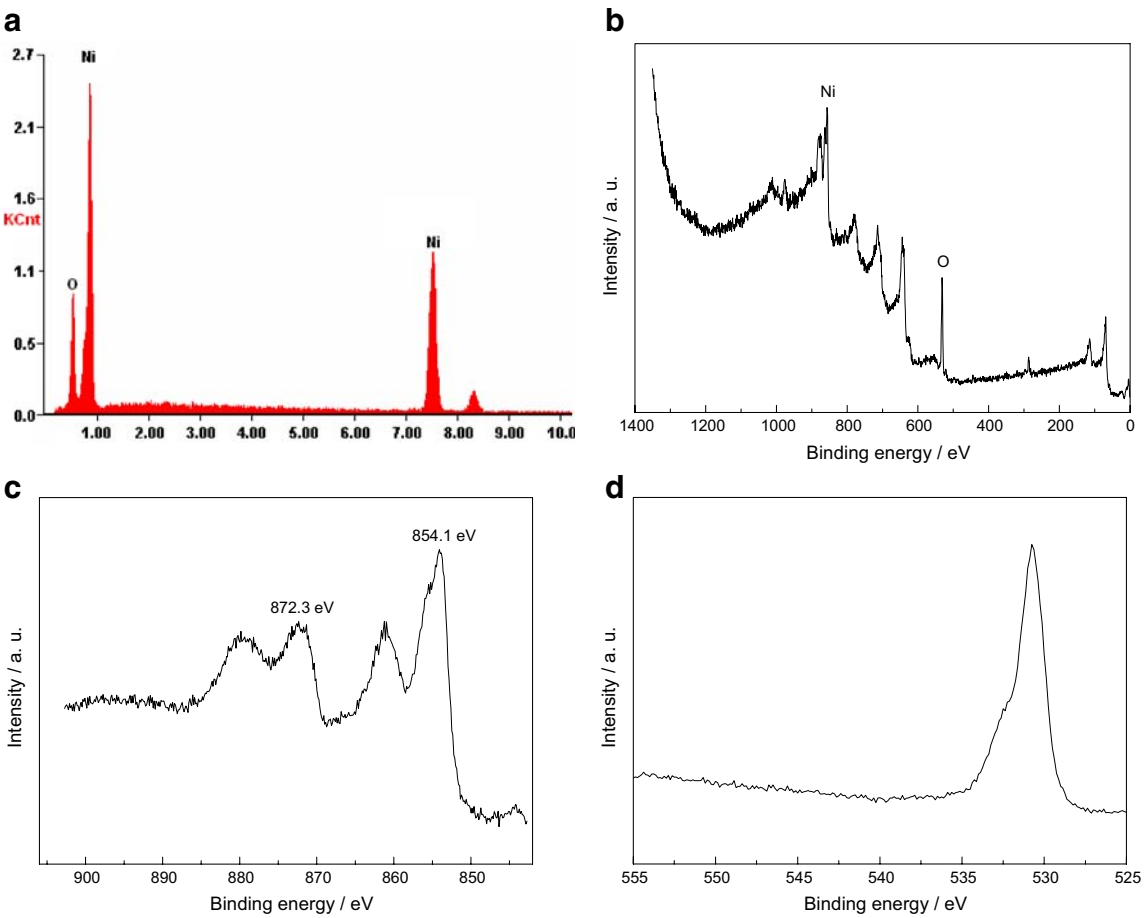

Fig. 1 EDAX (**a**) and XPS (**b**–**d**) spectra of the NiO films prepared at 500 °C; (**b**) survey spectrum, (**c**) Ni 2p and (**d**) O 1s

Results and discussion

At first, energy dispersive X-ray spectroscopy (EDX) was employed to identify the composition of the films prepared at 500 °C (Fig. 1). EDX result reveals that the films consist of nickel and oxygen, whereas no other elements, including nitrogen, potassium or sulfur, are detectable. The atom contents of Ni and O are 54.03% and 45.97%, respectively, which is close to the formula of NiO. Further experiments with X-ray photoelectron spectroscopy (XPS) for high-resolution scan of Ni 2p find the binding energy peaks of $2p_{3/2}$ at 854.1 eV and $2p_{1/2}$ at 872.3 eV (Fig. 1c), revealing the energy state of only Ni^{2+}. The element concentrations of Ni and O are 51.02% and 48.98%, respectively, implying the existence of NiO compound.

Figure 2 shows SEM images of the NiO film deposited on a foam nickel substrate. As seen in Fig. 2, the NiO film is composed of nanoribbons and these nanoribbons connect each other to form nanopits of a few hundred nanometers in diameter, displaying a highly porous appearance. It is reasonable that these porous morphologies will greatly enlarge electrolyte/electrode contact area and shorten diffusion path for both Li ions and electrons. So EDX, XPS, and SEM analysis confirm that porous films consisting of NiO nanoribbons had been deposited on foam nickel substrates.

The formation of NiO nanoribbons on a foam nickel substrate includes a simple oxidation–dehydration process, and the mechanism can be illustrated by following equations.

$$Ni + 2NH_3 + K_2S_2O_8 + 2H_2O \rightarrow Ni(OH)_2 + (NH_4)_2SO_4 + K_2SO_4 \quad (1)$$

$$Ni(OH)_2 \rightarrow NiO + H_2O \quad (2)$$

This deposition mechanism is similar to the growth of CuO nanoribbon and nanofiber from the aqueous solution contained $K_2S_2O_8$ and NaOH reported in the literatures [21, 22].

To evaluate the electrochemical performance of the NiO films prepared at 500 °C, cyclic voltammograms were recorded over the potential range of 0–3.0 V, as shown in Fig. 3a. A strong cathodic peak centers at 0.18 V during the first scan. The peak relates to the reactions including the reduction of NiO into Ni, and the formation of solid electrolyte interface (SEI) film and amorphous Li_2O. In the subsequent charge process, only one anodic peak locates at about 2.25 V, which can be attributed to the decomposition of the SEI film and the reaction between Ni and Li_2O, respectively [23, 24]. After the initial scan, the cathodic peak shifts to more positive potential and its intensity decreases significantly. The CV peaks show very good reproducibility after the first scan cycle.

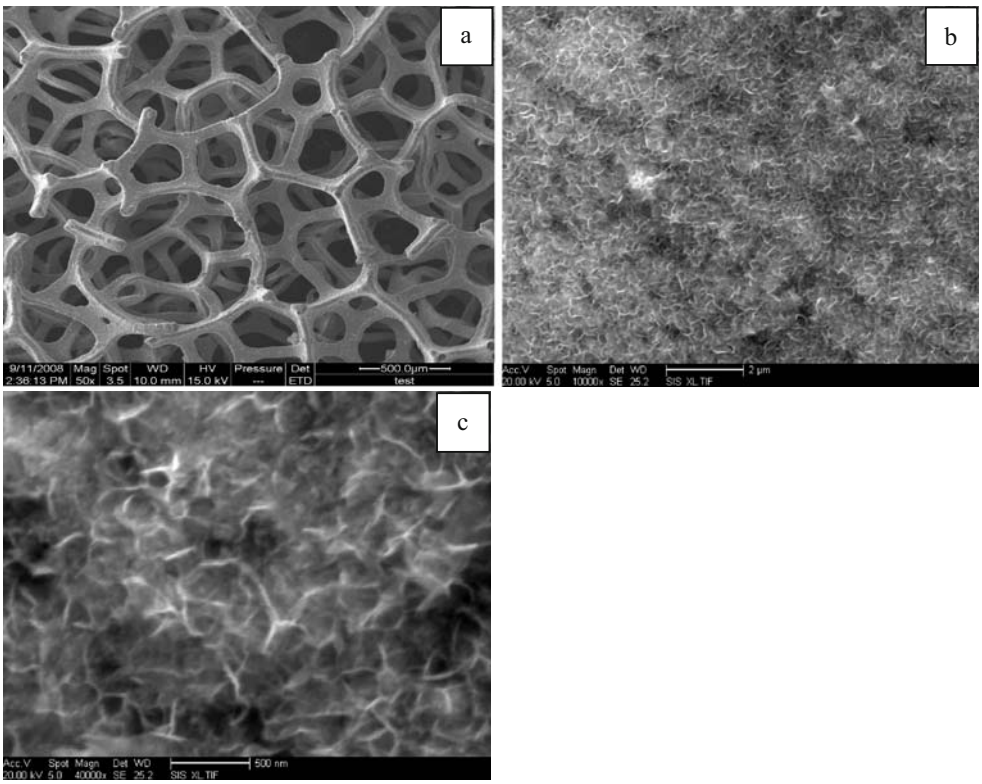

Fig. 2 SEM images of the NiO films calcined at 500 °C

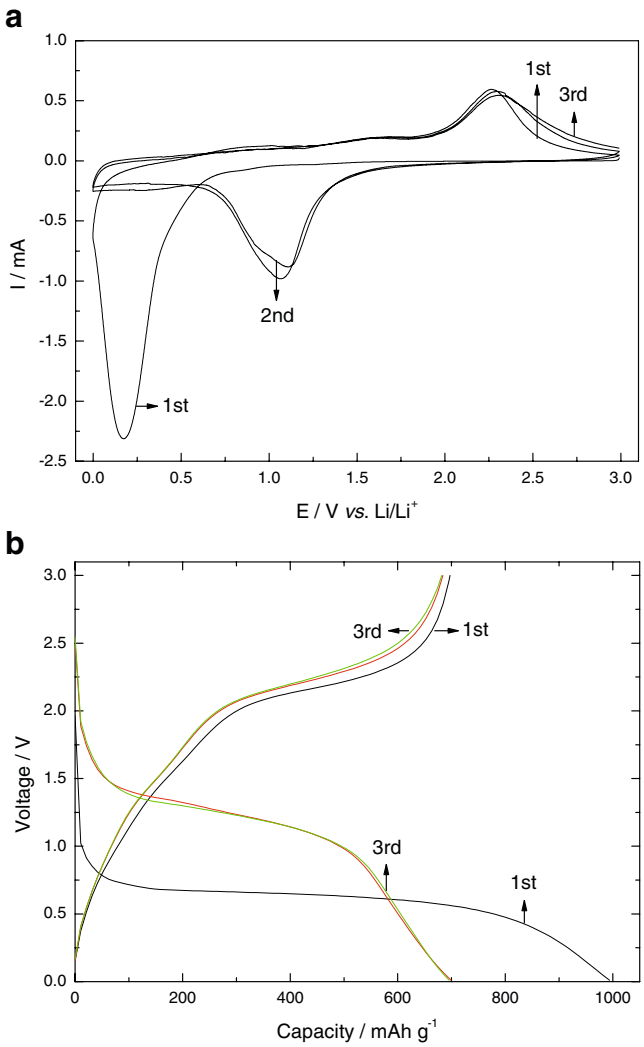

Fig. 3 Cyclic voltammograms (**a**) and voltage–capacity profiles (**b**) of the NiO films prepared at 500 °C

Figure 3b is the voltage/capacity profile of the NiO films in the first three discharge/charge cycles at 0.25C (1C= 718 mA g^{-1}). During the first discharge, Fig. 3b exhibits a distinct plateau at 0.70 V, followed by a gradual slope. The total capacity for the first discharge reaches 994 mAh g^{-1}. Subsequent charge curve shows a large voltage hysteresis, indicating a conversion mechanism [3, 7]. A capacity of 695 mAh g^{-1} is delivered for the first charge process and the NiO electrodes show a coulombic efficiency of 69.9%. Therefore, the NiO films reported here show a reversible capacity close to 1.8 times of the graphite (372 mAh g^{-1}).

After the initial discharge/charge cycle, the capacity of the films is very stable in the subsequent cycles. Figure 4a shows the cycling characteristics of the NiO films at 1 C. It is observed that they are able to maintain a capacity of 558 mAh g^{-1} even after 100 cycles, which is approximately 97% of the maximal charge capacity. For the purpose of comparison, we have compared reported samples. Under the same conditions, the reported NiO gave poor cyclability [14–19, 25–28]. Two comparable results are reported by Chiu et al. using reactive rf sputter deposition [29] and plasma assisted oxidation methods, respectively [30]. By

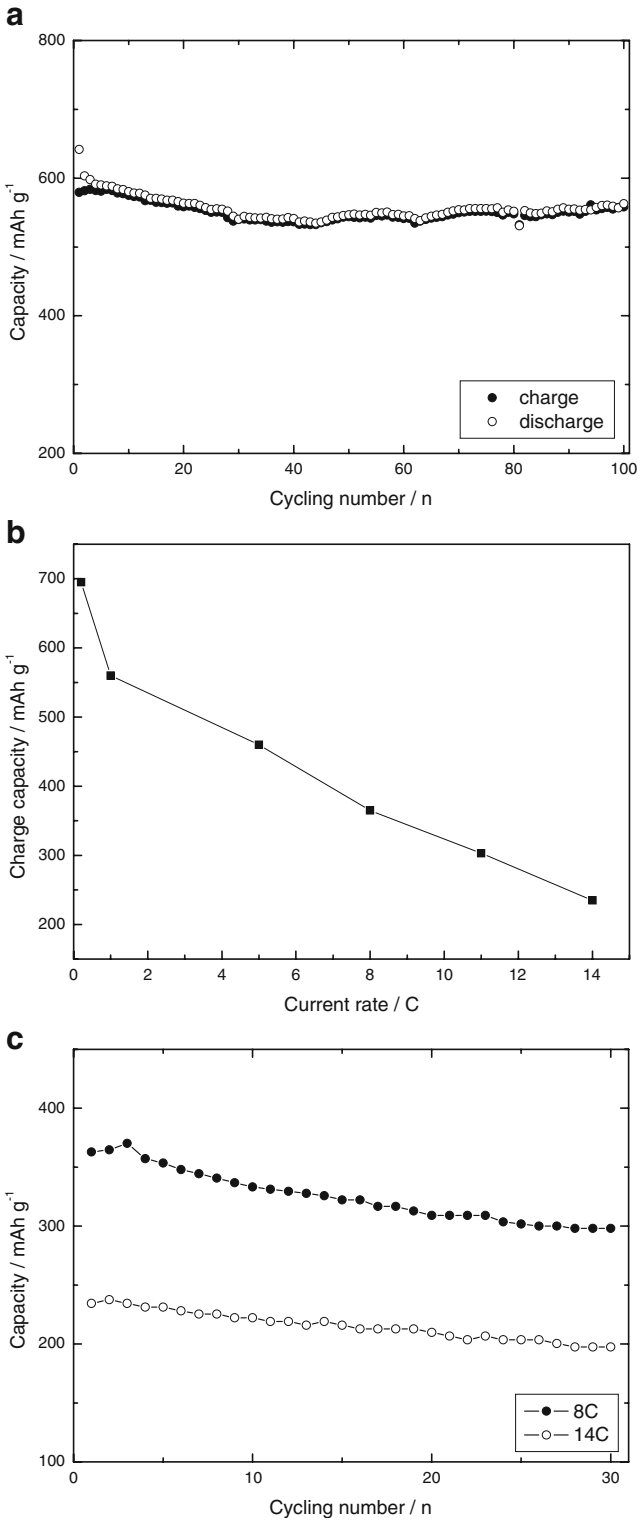

Fig. 4 Cycling characteristics (**a**) and rate capability (**b** and **c**) of the NiO films prepared at 500 °C

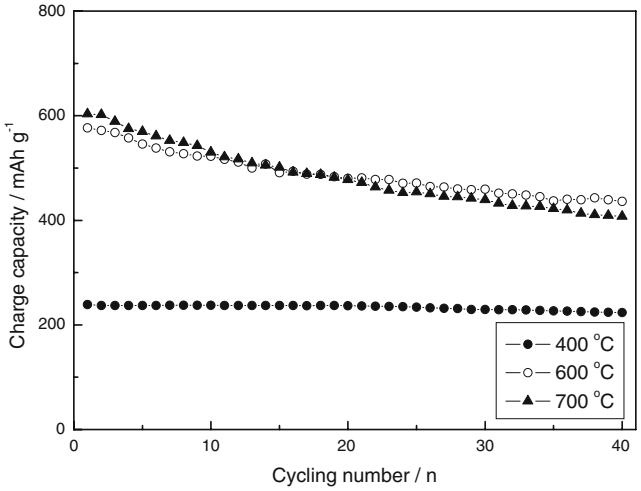

Fig. 5 Influence of calcination temperature on the electrochemical performance of NiO films, discharge/charge rate, 1.0C

comparison, it is easy to tell that our NiO films show one of the best capacity retention among the reported NiO anode materials. Of course, their capacity still fades, but we think this capacity fading is acceptable for practical application and it can be further ameliorated by optimizing fabrication conditions.

The NiO films also exhibit excellent rate capability, and the charge capacities at various discharge/charge rates are plotted in Fig. 4b. We can observe that the films can retain 82% charge capacity at 5C, 65% at 8C, and 42% at 14C relative to the capacity at 1C. Figure 4c shows the charge capacities of the first 30 cycles at 8C and 14C. After 30 cycles, the NiO electrodes still keep a capacity over 298 mAh g^{-1} at 8C and 197 mAh g^{-1} at 14C. In contrast, the capacity of the reported NiO samples decays much more sharply with the increase of current density [31–34]. Therefore, the rate capability of our NiO films surpasses most previously published results on NiO. The only comparable case is the mesoporous NiO formed on the nickel mesh and knitted nickel micron-wires via self-template method [35]. This is a very desirable feature for power source where high-rate discharge/charge capability is required.

We believe that the high reversibility and rate capability of the NiO films arise from their unique architectures. First, the porous morphology can ensure that every NiO nanoribbon is in electric contact with the foam nickel substrate and also interfaced with the electrolyte solution. Second, the open space between nanoribbons allows easy diffusion of the electrolyte into the inner region of the NiO films. Third, the films in this study are porous with a BET surface area of 45.1 m^2 g^{-1}, which enhance the electrolyte/NiO contact area, shorten the Li ion diffusion length, and accommodate the strain induced by the volume change during the lithium insertion–extraction process [36]. Finally, the foam nickel substrates act as electrical connectors to enhance the electrical contact between NiO nanoribbons, guaranteeing the electronic kinetics to take place. As a result, our NiO films can achieve high reversibility and rate capability.

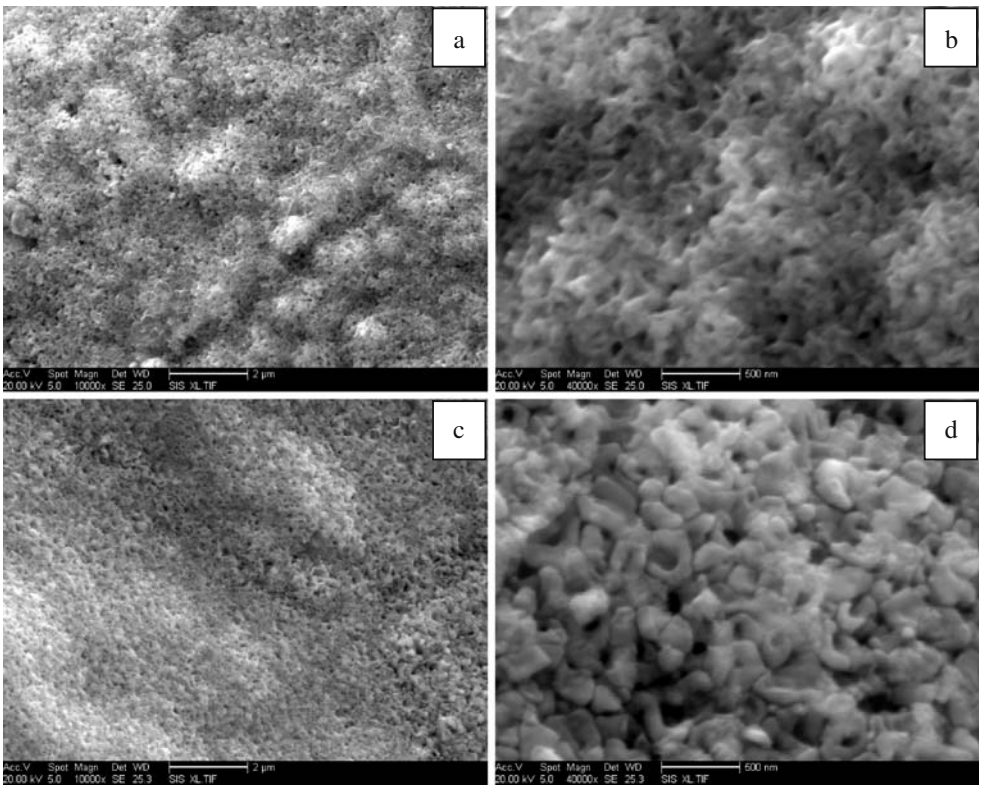

Fig. 6 SEM images of the NiO films prepared at 600 °C (**a** and **b**) and 700 °C (**c** and **d**)

The effect of calcination temperature on the morphologies and electrochemical properties of the NiO films was investigated furthermore. Scanning electron microscopy observations and electrochemical measurement reveal that the calcination temperature strongly influences the morphology of the films and results in different electrochemical performance. As shown in Fig. 5, the NiO film calcined at lower temperature exhibits lower capacity but better cyclability than those prepared at higher temperature. For example, at a rate of 1.0C, the film prepared at 400 °C delivers a capacity of 240 mAh g^{-1} and it keeps 93% of its initial value after 40 cycles; whereas that fabricated at 700 °C can only retain 67.7% of its initial capacity under the same conditions (though it exhibits an initial capacity as high as 603 mAh g^{-1}). The reversible capacity and cyclability of the film synthesized at 600 °C are between those of the two samples.

The difference in electrochemical performance is related to the morphology variation of the films, as illustrated in Fig. 6. The film calcined at 600 °C displays a porous morphology composed of nanoparticles. The size of particles further enlarges as the calcination temperature is increased to 700 °C, indicating the presence of heat-induced morphology change. These results confirm that the surface morphology of the NiO films has a strong impact on reversible capacity and capacity retention, which is consistent with the previous reports [25]. In addition to morphology change, the heat treatment will affect the crystallinity of the NiO films. For the film prepared at high temperature, well-crystallized NiO particles are formed. In this case, Li ions insertion is often accompanied by lattice structure distortion [37], leading to volume change and thereafter capacity fading upon discharge/charge cycles. Whereas for the film synthesized at lower temperature, its crystal structure is less well packed and thus possesses greater ability for structural accommodation.

Conclusions

In summary, a mild and simple method has been developed for fabricating three-dimensional NiO films on foam nickel substrates, and the resulting NiO films have shown high capacity, good cyclability, and excellent rate capability as the anodes of lithium-ion batteries. We believe that the outstanding performance of the NiO films arises from their large surface area, short and facile diffusion paths, and enhanced electrical contact. With their ease of fabrication on large-scale and excellent electrochemical performance, these NiO films may be favorable anodes for high-energy-density lithium-ion batteries.

Acknowledgement The work was supported by program of excellent team in Harbin Institute of Technology.

References

1. Kang K, Meng YS, Berger J, Grey CP, Ceder G (2006) Science 311:977, doi:10.1126/science.1122152
2. Chung SY, Blocking JT, Chiang YM (2002) Nat Mater 1:123, doi:10.1038/nmat732
3. Poizot P, Laruelle S, Grugeon S, Dupont L, Tarascon JM (2000) Nature 407:496, doi:10.1038/35035045
4. Tarascon JM, Armand A (2001) Nature 414:359, doi:10.1038/35104644
5. Arico S, Bruce P, Scrosati B, Tarascon JM, Schalkwijk TV (2005) Nat Mater 4:366, doi:10.1038/nmat1368
6. Wang Y, Takahashi K, Lee K, Cao G (2006) Adv Funct Mater 16:1133, doi:10.1002/adfm.200500662
7. Taberna PL, Mitra S, Poizot P, Simon P, Tarascon JM (2006) Nat Mater 5:567, doi:10.1038/nmat1672
8. Nam KT, Kim DW, Yoo PJ, Chiang CY, Meethong N, Hammond PT, Chiang YM, Belcher AM (2006) Science 312:885, doi:10.1126/science.1122716
9. Armstrong G, Armstrong AR, Bruce PG, Reale P, Scrosati B (2006) Adv Mater 18:2597, doi:10.1002/adma.200601232
10. Yoshio, Tadahiko K, Akihiro M, Yukio M, Tsutomu M (1997) Science 276:1395, doi:10.1126/science.276.5317.1395
11. Lee H, Cho J (2007) Nano Lett 7:2638, doi:10.1021/nl071022n
12. Moriguchi, Hidaka R, Yamada H, Kudo T, Murakami H, Nakashima N (2006) Adv Mater 18:69, doi:10.1002/adma.200501366
13. Yu Y, Chen CH, Shui JL, Xie S (2005) Angew Chem Int Edn 44:7085
14. Nuli YN, Zhao SL, Qin QZ (2003) J Power Sources 114:113, doi:10.1016/S0378-7753(02)00531-1
15. Wang Y, Qin QZ (2002) J Electrochem Soc 149:A873, doi:10.1149/1.1481715
16. Doh CH, Kalaiselvi N, Park CW (2004) Ionics 10:421, doi:10.1007/BF02378003
17. Needham SA, Wang GX, Liu HK (2006) J Power Sources 159:254, doi:10.1016/j.jpowsour.2006.04.025
18. Needham SA, Wang GX, Liu HK (2006) J Nanoscience Nanotech 6:77
19. Yuan L, Guo ZP, Konstantinov K (2006) Electrochem Solid-State Lett 9:A524, doi:10.1149/1.2345550
20. Chan CK, Peng H, Twesten RD, Jarausch K, Zhang XF, Cui Y (2007) Nano Lett 7:490, doi:10.1021/nl062883j
21. Wang HB, Pan QM, Zhao JW, Yin GP, Zuo PJ (2007) J Power Sources 167:206, doi:10.1016/j.jpowsour.2007.02.008
22. Hou HW, Xie Y, Li Q (2005) Cryst Growth Des 5:201, doi:10.1021/cg049972z
23. Debart, Dupont L, Poizot P, Leriche JB, Tarascon JM (2001) J Electrochem Soc 148:A1266, doi:10.1149/1.1409971
24. Grugeon S, Laruelle S, Herrera-Urbina R, Dupont L, Poizot P, Tarascon JM (2001) J Electrochem Soc 148:A285, doi:10.1149/1.1353566
25. Oh SW, Bang HJ, Bae YC, Sun YK (2007) J Power Sources 173:502, doi:10.1016/j.jpowsour.2007.04.087
26. Huang XH, Tu JP, Zhang B, Zhang CQ, Li Y, Yuan YF, Wu HM (2006) J Power Sources 161:541, doi:10.1016/j.jpowsour. 2006.03.039
27. Ni X, Zhang Y, Tian D, Zheng H, Wang X (2007) J Cryst Growth 306:418, doi:10.1016/j.jcrysgro.2007.05.013
28. Wang X, Li L, Zhang YG et al (2006) Cryst Growth Des 6:2163, doi:10.1021/cg060156w

29. Chiu KF, Chang CY, Lin CM (2005) J Electrochem Soc 152: A1188, doi:10.1149/1.1906024
30. Varghese B, Reddy MV, Zhu Y (2008) Chem Mater 20:3360, doi:10.1021/cm703512k
31. Huang XH, Tu JP, Zhang CQ, Xiang JY (2007) Electrochem Commun 9:1180, doi:10.1016/j.elecom.2007.01.014
32. Huang XH, Tu JP, Zhang CQ, Chen XT, Yuan YF, Wu HM (2007) Electrochim Acta 52:4177, doi:10.1016/j.electacta.2006.11.034
33. Wang Y, Zhang YF, Liu HR, Yu SJ, Qin QZ (2003) Electrochim Acta 48:4253, doi:10.1016/S0013-4686(03)00612-1
34. Huang XH, Tu JP, Zeng ZY, Xiang JY, Zhao XB (2008) J Electrochem Soc 155:A438, doi:10.1149/1.2904878
35. Hosono E, Fujihara S, Honma I, Zhou H (2006) Electrochem Commun 8:284, doi:10.1016/j.elecom.2005.11.023
36. Li Y, Tan B, Wu Y (2008) Nano Lett 8:265, doi:10.1021/nl0725906
37. Morales J, Sanchez L, Tirado JL (1998) J Solid State Electrochem 2:420, doi:10.1007/s100080050120